

# Monte Carlo dosimetry of a new $^{90}\text{Y}$ brachytherapy source

Wu Junxiang, ME<sup>1</sup>, You Shihu, ME<sup>1</sup>, Huang Jing, ME<sup>1</sup>, Long Fengxiang, ME<sup>1</sup>, Wang Chengkai, ME<sup>2</sup>, Prof. Wu Zhangwen<sup>1</sup>, Prof. Hou Qing<sup>1</sup>, Prof. Gou Chengjun<sup>1</sup>

<sup>1</sup>Key Laboratory of Radiation Physics and Technology, Ministry of Education and Institute of Nuclear Science and Technology, Sichuan University, <sup>2</sup>College of Chemistry, Sichuan University, Chengdu Sichuan 610064, China

## Abstract

**Purpose:** In this study, we attempted to obtain full dosimetric data for a new  $^{90}\text{Y}$  brachytherapy source developed by the College of Chemistry (Sichuan University) for use in high-dose-rate after-loading systems.

**Material and methods:** The dosimetric data for this new source were used as required by the dose calculation formalisms proposed by the AAPM Task Group 60 and Task Group 149. The active core length of the new  $^{90}\text{Y}$  source was increased to 4.7 mm compared to the value of 2.5 mm for the old  $^{90}\text{Sr}/^{90}\text{Y}$  source. The Monte Carlo simulation toolkit Geant4 was used to calculate these parameters. The source was located in a 30-cm-radius theoretical sphere water phantom.

**Results:** The dosimetric data included the reference absorbed dose rate, the radial dose function in the range of 1.0 to 8.0 mm in the longitudinal axis, and the anisotropy function with a  $\theta$  in the range of  $0^\circ$  to  $90^\circ$  at  $5^\circ$  intervals and an  $r$  in the range of 1.0 to 8.0 mm in 0.2-mm intervals. The reference absorbed dose rate for the new  $^{90}\text{Y}$  source was determined to be equal to  $1.6608 \pm 0.0008 \text{ cGy s}^{-1} \text{ mCi}^{-1}$ , compared to the values of  $0.9063 \pm 0.0005 \text{ cGy s}^{-1} \text{ mCi}^{-1}$  that were calculated for the old  $^{90}\text{Sr}/^{90}\text{Y}$  source. A polynomial function was also obtained for the radial dose function by curve fitting.

**Conclusions:** Dosimetric data are provided for the new  $^{90}\text{Y}$  brachytherapy source. These data are meant to be used commercially in after-loading system.

J Contemp Brachytherapy 2015; 7. 5: 397-406

DOI: 10.5114/jcb.2015.55362

**Key words:**  $^{90}\text{Y}$  source, brachytherapy, dosimetry, Geant4, Monte Carlo.

## Purpose

Currently, many new types of brachytherapy sources are available. Beta-emitting sources are widely utilized in brachytherapy fields. The dosimetric parameters of beta-emitting sources that have been applied in intravascular brachytherapy (IVBT) have been calculated through some experimental measurements and various simulation programs. For example, Soares *et al.* obtained a radial dose function and an anisotropy function from their measurements of an old  $^{90}\text{Sr}/^{90}\text{Y}$  source in A150 plastic, and these authors also presented Monte Carlo results of these dosimetric parameters [1]. The dosimetric parameters of an old  $^{90}\text{Sr}/^{90}\text{Y}$  source were calculated by Holmes *et al.* using an experimental method [2].

Furthermore, beta-emitting brachytherapy sources have been applied in radiotherapy for other localized tumors.  $^{90}\text{Y}$  microspheres have recently been used to treat unresectable hepatocellular cancer by Nelson *et al.* [3]. The  $^{32}\text{P}$  source model RIC-100 has been used for temporary radiation therapy of the spinal dura and other localized tumors, and dosimetric evaluations have been

applied to the source with an MCNP5 Monte Carlo code by Cohen *et al.* [4].

Recently, a new  $^{90}\text{Y}$  source was developed by Wang *et al.* (Sichuan University) that is a beta-particle-emitting source for treatment of liver cancer. According to the American Association of Physicists in Medicine (AAPM) TG60/TG149 report recommendations [5, 6], the dosimmetries at distances of one millimeter from the beta-emitting sources are poorly understood, and better understanding of the dosimetry in the millimeter range will help these sources in the development of clinical practice. All beta-emitting brachytherapy sources for use in clinical practice require obtaining dosimetric parameters based on the TG60/TG149 formalism. In addition, the TG60 and TG149 reports reviewed the physics of the IVBT and provided the dose parameter formalisms for the beta-emitting brachytherapy source. These dose parameters include the reference absorbed dose rate, radial dose function, and anisotropy function. However, the dosimetric parameters of the  $^{90}\text{Y}$  source have created new challenges in the field of brachytherapy dosimetry. The experimental measurements are difficult to perform accurately at these

**Address for correspondence:** Prof. Gou Chengjun, Institute of Nuclear Science and Technology, Sichuan University, No. 24 South Section 1, Yihuan Road, Chengdu, 610064, China, phone: +86 13219873330, fax: +86 028 85410252, e-mail: Cheng.J.Gou@263.net

Received: 19.06.2015

Accepted: 10.10.2015

Published: 31.10.2015

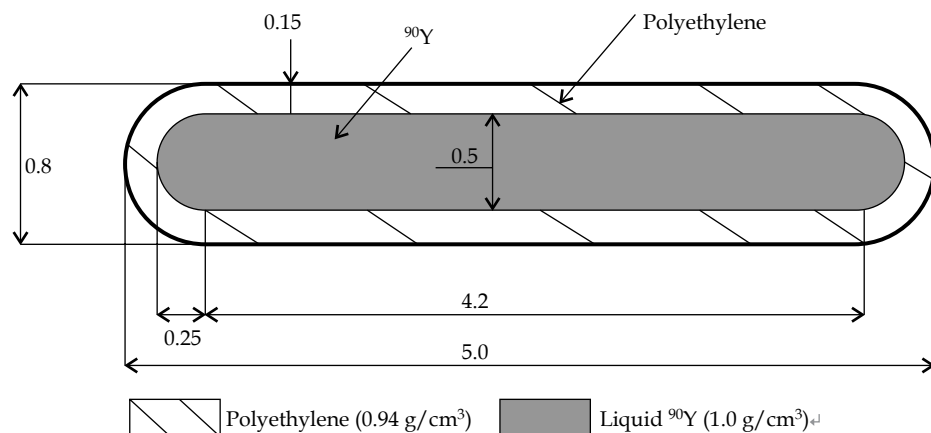


**Fig. 1.** Longitudinal view of new  $^{90}\text{Y}$  (mm)

close distances due to the large dose gradients and other technical considerations. When an experimental method does not work in the spatial scale of a millimeters or submillimeters, Monte Carlo methods can provide dosimetric data with the required spatial resolution [5, 7, 8]. Monte Carlo methods play important roles in dosimetry and radiotherapy, especially regarding the performance of difficult radiation transport problems [9]. In the present work, we employed the Monte Carlo simulation code Geant4 to derive accurate calculations of the dosimetric parameters of the new  $^{90}\text{Y}$  source according to the dose calculation formalisms recommended by AAPM reports TG60/TG149 and the quality assurance (QA) purposes of the new  $^{90}\text{Y}$  source. The reference absorbed dose rate and radial dose functions were compared with the results of the old  $^{90}\text{Sr}/^{90}\text{Y}$  source calculated by Wang *et al.* [8].

## Material and methods

### Brachytherapy sources

The source design, materials and sizes are presented in Figure 1. The design of the new  $^{90}\text{Y}$  source was provided by the College of Chemistry (Sichuan University), and the tolerances of this new source were  $\pm 0.01$  mm provided by manufacturer. The basic sizes and materials of the core and capsules used in the simulation were taken as follows: the composition of the liquid  $^{90}\text{Y}$  core was assumed to be  $\text{H}_2\text{O}$  with a density of  $1.0 \text{ g/cm}^3$ , and the radioactive material was uniformly distributed in its core. The active core was encapsulated. The capsule material was polyethylene (PE, 86% carbon and 14% hydrogen) with an effective density of  $0.94 \text{ g/cm}^3$  as shown in Table 1. The active length of the new source was 4.7 mm. At the

center of the capsule was a cylinder 4.2 mm in length, 0.8 mm in outer diameter, and 0.5 mm in inner diameter, with two semispherical endings with 0.8 mm external diameters and 0.5 mm inner diameters on the top and the bottom of the cylindrical capsule. The thickness of the PE capsule was 0.15 mm at the cylindrical core.

The  $^{90}\text{Y}$  source was a pure beta emitter with a 2.7-day half-life, a maximum beta energy of 2.288 MeV, and an average beta energy of 0.934 MeV [5, 10]. The energy spectrum of the  $^{90}\text{Y}$  source was complicated and has been described by Cross *et al.* [11]; the values of the  $^{90}\text{Y}$  energy spectrum are presented in Table 2 [11]. Additionally, many other beta-emitting brachytherapy sources are available ( $^{90}\text{Sr}$ ,  $^{32}\text{P}$ , and  $^{90}\text{Sr}/^{90}\text{Y}$  source).  $^{90}\text{Sr}$  source with a 28.5 years half-life, an average and a maximum energies of 196 keV and 546 keV, respectively [10]. The  $^{32}\text{P}$  source is a pure beta emitter with a 14.3 day half-life, a maximum beta energy of 1.71 MeV and an average beta energy of 0.695 MeV [12]. The  $^{90}\text{Sr}/^{90}\text{Y}$  source emitted electrons with energies in a continuum that reached up to

**Table 2.** Nuclear data for the  $^{90}\text{Y}$  source

Half-life/d	Electron energy (MeV)	Electrons per disintegration
2.7	0.0	0.3131
	0.2288	0.4101
	0.4576	0.5204
	0.6864	0.5970
	0.9152	0.6215
	1.1441	0.5990
	1.3729	0.5199
	1.6017	0.4097
	1.8305	0.2702
	2.0593	0.1269
	2.2880	0.0001

**Table 1.** Chemical composition of materials by percentage mass fraction

Material	Elements	Density (g/cm <sup>3</sup> )	Composition (% weight)
Polyethylene (PE)	C H	0.94	0.8563 0.1437

2.2 MeV [11]. Compared to the commonly used beta-emitter brachytherapy sources, the new  $^{90}\text{Y}$  source had a much shorter half-life than the common beta-emitting sources with the aim of providing increased flexibility and radiation safety. Additionally, the new  $^{90}\text{Y}$  source had a greater energy, this high energy makes the radiation more penetrating while having a sharper slope of the depth dose. Because of these features and due to the high-purity decay of betas,  $^{90}\text{Y}$  seems a more suitable radionuclide for an effective treatment [10].

### Dose calculation formalism

The dose calculation formalism for the beta-emitting source proposed by the AAPM report TG60 in 1999 was followed. This formalism is described in terms of the polar coordinate system as shown in Figure 2. For a beta-particle-emitting source, the dose calculation formalism is different from that for a photon-emitting source. The air kerma strength ( $S_k$ ) and dose rate constant in water ( $\Lambda$ ) were replaced by the reference absorbed dose rate  $D(r_0, \theta_0)$ , which has units of  $\text{cGy s}^{-1} \text{ mCi}^{-1}$ . This replacement occurred because the air kerma was only applied to photon emitting sources and did not exist for beta-emitting sources [5]. The dose at any point around the source can be expressed as follows:

$$D(r, \theta) = D(r_0, \theta_0) \times \frac{G_L(r, \theta)}{G_L(r_0, \theta_0)} \times g_L(r) \times F(r, \theta) \quad (1)$$

where  $L$  is the active length of the source ( $L = 4.7 \text{ mm}$ ) and  $r_0$  is the reference distance, which was defined as  $2 \text{ mm}$  in this protocol. The reference angle  $\theta_0$  was specified as  $\pi/2$ .  $G_L(r, \theta)$  is the geometry factor,  $g_L(r)$  is the radial dose function (the subindex L means the use of the 2D approach instead the 1D), and  $F(r, \theta)$  is the dose anisotropy function.

### Monte Carlo simulation code

We used Monte Carlo Geant4 methods to study the dosimetric parameters of the new  $^{90}\text{Y}$  source. The Monte Carlo methods were particle of transport methods that have increasingly been used in radiation therapy, mainly in the development of the brachytherapy field. Popular Monte Carlo methods in this field include Geant4 [13], FLUKA [14], EGS [15], MCNP [16], and PENELOPE [17]. The Geant4 code has been developed and successfully applied in the high, a low energy ranges, and beta-emitting brachytherapy sources [18].

Geant4 (Geant4.9.6.P02 development version) was developed by the European Organization for Nuclear Research (CERN) and is based on the C++ language. This code exploits advanced software-engineering techniques and object-oriented technology to achieve transparency, and requires the user to write each particle and physics model for inclusion in the simulation. This software also provides interaction models for all of the electromagnetic and nuclear processes that are relevant to the transport of brachytherapy. The Geant4 physics model selected for this work was a standard electromagnetic interaction

model and employed the function GetTotalEnergyDeposit to obtain the dosimetric data. The Geant4 photon and electron cross sections were based on the EPDL97 and EEDL97 cross section libraries, respectively [19, 20]. The number of electrons  $N_e$  generated in each simulation was  $N_e = 3 \times 10^8$ , and the cutoff energy of photon and electron was set to 1 keV [21]. In the results for the new  $^{90}\text{Y}$  source, all of the secondary particles generated by the source particles (electrons and photons) were completed scored.

In this study, we assumed that the new  $^{90}\text{Y}$  source was positioned at the center of a spherical liquid water phantom with a  $30 \text{ cm}$  radius, which was performed to provide dose data for water and to simulate infinite phantom conditions for distances of  $r < 10 \text{ mm}$ . The absorbed dose that was used to calculate the radial dose function and anisotropy function was obtained simultaneously in cylindrical ( $y, z$ ) and spherical ( $r, \theta$ ) coordinates, and the source axis is along the  $z$  axis of the coordinate system as shown in Figure 2. In the coordinate system,  $y$  and  $z$  are representative of the radial and axial coordinates, respectively. In the spherical coordinates,  $r$  is defined as the distance from the center of the active region of the source. When  $z = 0$ , we set up the scoring cells at  $y$  in the range from  $1.0$  to  $8.0 \text{ mm}$  in  $0.2\text{-mm}$  intervals to obtain the absorbed dose  $D(y, z)$ . Subsequently, we used these absorbed doses to obtain the radial dose function. In the spherical coordinate system, we set up the scoring cells at the same distances as those used in the cylindrical coordinate system. Simultaneously, we used  $\theta$  ranges from  $0^\circ$  to  $90^\circ$  in  $5^\circ$  intervals to obtain the absorbed dose  $D(r, \theta)$  and then used the anisotropy function equation to calculate the anisotropy function.

### Uncertainty analysis

According to AAPM TG-43U1 recommendation, a dosimetric uncertainties (statistical uncertainty and systematic uncertainty) analysis should be performed [22]. We used Monte Carlo Geant4 absorbed dose  $D(y, z)$  over the range of  $0.0 \text{ mm} \leq y \leq 8.0 \text{ mm}$ ,  $0.0 \text{ mm} \leq z \leq 8.0 \text{ mm}$ , and statistical uncertainty equation to obtain statistical uncertainty (type A). For the new  $^{90}\text{Y}$  source, the statistical uncertainty of the Monte Carlo dose  $D(y, z)$  depended on the axial position  $z$  and the radial position  $y$ . When  $z \leq 4 \text{ mm}$ , the statistical uncertainty was within  $0.48\%$  for  $y \leq 8 \text{ mm}$ . With increases in the position  $z$  ( $4 \text{ mm}$

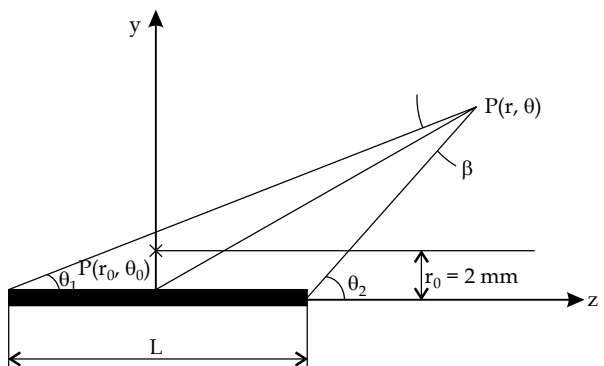


Fig. 2. Polar coordinate system for the dose calculation

$\leq z \leq 8$  mm), the statistical uncertainty was within 2.7% for  $y \leq 8$  mm.

Systematic uncertainty (type B) for the new  $^{90}\text{Y}$  source based on Monte Carlo simulation. The component of systematic uncertainty included source geometry, capsule geometry, phantom composition, and cutoff energy as shown in Table 3. 1. Tolerances of  $\pm 0.01$  mm on the new  $^{90}\text{Y}$  source diameter and capsule thickness were provided by the manufacturer. For  $+0.01$  and  $-0.01$  mm on the new  $^{90}\text{Y}$  source diameter, these would cause 0.007% and 0.004% variations in  $D(2\text{ mm}, \theta_0)$ , respectively. For  $+0.01$  and  $-0.01$  mm on the capsule thickness, these would cause variations in  $D(2\text{ mm}, \theta_0)$  of 0.882% and 0.858%, respectively. 2. Systematic uncertainty in water and air phantom compositions and mass densities were calculated to result in  $D(2\text{ mm}, \theta_0)$  of 3.862%. 3. Given the 1 keV and 10 keV cutoff energy for  $D(2\text{ mm}, \theta_0)$ , and the uncertainties was 0.877%.

## Results

### Reference absorbed dose rate

The reference absorbed dose at point  $r_0 = 2$  mm for the new  $^{90}\text{Y}$  source was obtained by using the Geant4 code and it was found to be equal to  $4.4887 \times 10^{-10}$  Gy/electron. The reference absorbed dose rate  $D(r_0, \theta_0)$  of the new  $^{90}\text{Y}$  source in water was  $1.6608 \text{ cGy s}^{-1} \text{ mCi}^{-1}$  as shown in Table 4, which also illustrates the values that were calculated for the old  $^{90}\text{Sr}/^{90}\text{Y}$  source by Wang *et al.* [8] using a EGS4 Monte Carlo code (the composition of the capsule was SS304 stainless steel and the diameter and height of the active core were 0.56 and 2.5 mm, respectively). The value of  $D(r_0, \theta_0)$  for the new  $^{90}\text{Y}$  source was 45% higher than that calculated for the old  $^{90}\text{Sr}/^{90}\text{Y}$  source and these percentage differences were nearly equal to the percentage differences observed for the energies, sizes, and materials for the two sources. The new  $^{90}\text{Y}$  source

**Table 3.** Systematic uncertainty for the new  $^{90}\text{Y}$  source

Component	$D(2\text{ mm}, \theta_0)$	
	Type B (%)	
Source geometry ( $\pm$ )	0.007%	
	0.004%	
Capsule geometry ( $\pm$ )	0.882%	
	0.858%	
Phantom composition	3.862%	
Cutoff energy	0.877%	

**Table 4.** Absorbed dose rate at reference

Source	$D(r_0, \theta_0)$	Unit
New $^{90}\text{Y}$	$1.6608 \pm 0.0008$	$\text{cGy s}^{-1} \text{ mCi}^{-1}$
Old $^{90}\text{Sr}/^{90}\text{Y}$	$0.9063 \pm 0.0005$	$\text{cGy s}^{-1} \text{ mCi}^{-1}$

had a greater energy than the old  $^{90}\text{Sr}/^{90}\text{Y}$  source and this high energy makes the radiation more penetrating.

### Radial dose functions

The two-dimensional dose distribution  $D(r_0, \theta_0)$  was calculated for the new  $^{90}\text{Y}$  source in water. This dose distribution was used to derive the radial dose functions of the source. Table 5 shows the radial dose function  $g_L(r)$  at the radial distances over the range of 1.0 to 8.0 mm (the subindex L means the use of the 2D approach instead the 1D with active length  $L = 4.7$  mm). This table illustrates that, at the radial distances far from the source ( $r \geq 8.0$  mm), the radial dose functions had lower values.

In Figure 3, a fitted polynomial function of the new  $^{90}\text{Y}$  source and a comparison of the radial dose functions

**Table 5.** Comparison of the radial dose function from this work to calculated values from other author

$r$ (mm)	$g_L(r)$ (this work)	Ref. 8
1.0	1.1368	1.0990
1.2	1.1030	
1.4	1.0862	
1.5	1.0600	1.0660
1.6	1.0672	
1.8	1.0337	
2.0	1.0000	1.0000
2.2	0.9775	
2.4	0.9521	
2.5	0.9245	0.9070
2.6	0.9002	
2.8	0.8750	
3.0	0.8381	0.7990
3.2	0.8015	
3.4	0.7628	
3.6	0.7219	
3.8	0.6769	
4.0	0.6331	0.5640
4.2	0.5872	
4.4	0.5469	
4.6	0.5075	
4.8	0.4695	
5.0	0.4323	0.3510
6.0	0.2631	0.1890
7.0	0.1272	0.0850
8.0	0.0454	0.0300

of the new <sup>90</sup>Y and the old <sup>90</sup>Sr/<sup>90</sup>Y source calculated according to EGS4 from Wang *et al.* [8], and the differences between two sources at right ordinate axis are presented. The comparison between two sources revealed the following: (a) at the radial distances of  $r \leq 2.0$  mm, our calculated  $g_L(r)$  values agreed with the calculations of Wang *et al.*'s within 3.3%; (b) for  $2.0 \text{ mm} \leq r \leq 4.0$  mm, differences between our calculations and those of Wang *et al.* were greater than 11%; and (c) for  $4.0 \text{ mm} \leq r \leq 8.0$  mm, our calculations were greater than those of Wang *et al.* by up to 34%. These results confirm that the different active core and geometry of the source dose significantly affected the values of the radial dose functions. These differences were due to the average energies, sizes, and materials of the two sources (our new <sup>90</sup>Y source had a greater energy than Wang *et al.*'s old <sup>90</sup>Sr/<sup>90</sup>Y source according to their energy spectrum and the values of the reference absorbed dose rate; the length of the active core was 4.7 mm rather than 2.5 mm and the material of the capsule was PE, rather than stainless steel).

The radial dose function  $g_L(r)$ , also fit over the range of  $1.0 \text{ mm} \leq r \leq 8.0 \text{ mm}$  using a fifth-order polynomial function as presented in Figure 3. The polynomial function is shown in Eq. (2). The values of the fitted parameters were as follows: R-squared ( $R^2$ ) 0.99992,  $a_0 = -0.00063$ ,  $a_1 = 0.05057$ ,  $a_2 = -0.37012$ ,  $a_3 = 6.84190$ ,  $a_4 = -15.69895$ ,  $a_5 = 8.42267$ , and  $a_6 = 1.7092$ . The overall accuracies of the fits were excellent, and the fits based on the polynomial exhibited maximum and mean deviations of less than 0.56% and 0.23%, respectively.

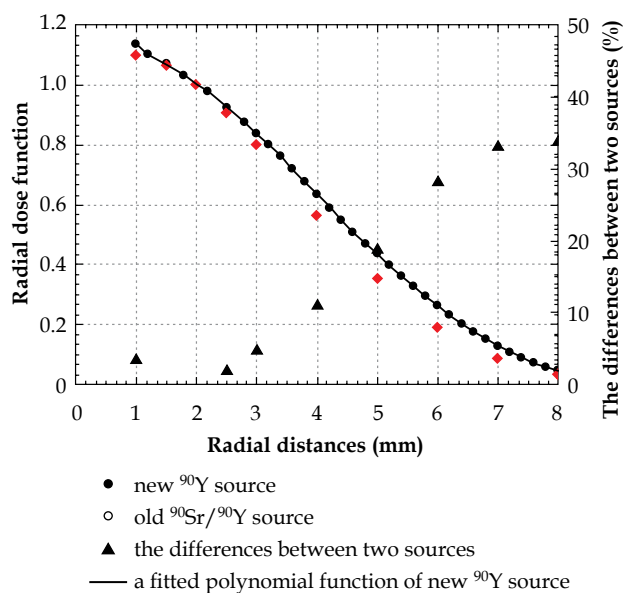


Fig. 3. Radial dose functions calculated for the new <sup>90</sup>Y source and the old <sup>90</sup>Sr/<sup>90</sup>Y source. The line is the polynomial fit of order 5 for the new <sup>90</sup>Y source

$$g(r) = (a_0 r^{-2} + a_1 r^{-1} + a_2 + a_3 r + a_4 r^2 + a_5 r^3) e^{-a_6 r} \quad (2)$$

where  $r$  is the radial distance from the center of the source for  $\theta = 0^\circ$ .

Table 6. Anisotropy function calculated for the new <sup>90</sup>Y source

Angle (°)	Radial distance (mm)									
	1.0	1.2	1.4	1.6	1.8	2.0	2.2	2.4	2.6	2.8
0									0.826	0.978
5									0.945	1.018
10								1.054	1.069	1.075
15				1.091	1.085	1.124	1.081	1.067	1.095	1.108
20		1.125	1.089	1.082	1.076	1.077	1.059	1.067	1.104	1.118
25	1.069	1.065	1.050	1.050	1.053	1.061	1.050	1.065	1.102	1.114
30	1.041	1.036	1.033	1.036	1.041	1.050	1.042	1.057	1.093	1.105
35	1.018	1.024	1.022	1.027	1.032	1.041	1.033	1.048	1.081	1.090
40	1.009	1.015	1.015	1.018	1.024	1.033	1.025	1.039	1.069	1.077
45	1.000	1.004	1.004	1.007	1.011	1.020	1.010	1.020	1.048	1.050
50	0.997	1.001	1.000	1.003	1.006	0.969	0.824	1.011	1.037	1.039
55	0.994	0.995	0.988	0.989	1.069	1.045	1.022	1.021	1.036	1.026
60	1.000	0.998	0.989	0.990	1.074	1.042	1.018	1.018	1.033	1.024
65	0.994	0.991	0.997	1.062	1.035	1.032	1.013	1.014	1.030	1.022
70	0.993	0.990	0.996	1.062	1.028	1.024	1.004	1.005	1.021	1.012
75	0.996	0.996	1.000	1.070	1.029	1.024	1.003	1.004	1.020	1.011

**Table 6.** Cont.

Angle (°)	Radial distance (mm)									
	1.0	1.2	1.4	1.6	1.8	2.0	2.2	2.4	2.6	2.8
80	0.998	1.010	1.020	1.081	1.039	1.035	1.016	1.018	1.035	1.027
85	1.041	1.066	1.068	1.141	1.085	1.078	1.060	1.063	1.082	1.075
90	1.000	1.000	1.000	1.000	1.000	1.000	1.000	1.000	1.000	1.000

Angle (°)	Radial distance (mm)									
	3.0	3.2	3.4	3.6	3.8	4.0	4.2	4.4	4.6	4.8
0	1.031	1.065	1.083	1.099	1.129	1.149	1.187	1.226	1.257	1.277
5	1.058	1.082	1.103	1.121	1.147	1.168	1.194	1.221	1.246	1.269
10	1.094	1.116	1.132	1.149	1.172	1.193	1.215	1.241	1.265	1.287
15	1.123	1.140	1.154	1.171	1.190	1.214	1.231	1.253	1.267	1.289
20	1.130	1.143	1.153	1.167	1.188	1.206	1.225	1.243	1.261	1.275
25	1.127	1.136	1.146	1.159	1.177	1.193	1.211	1.230	1.244	1.258
30	1.114	1.125	1.134	1.145	1.160	1.176	1.194	1.209	1.222	1.237
35	1.099	1.108	1.117	1.127	1.141	1.158	1.173	1.186	1.197	1.206
40	1.083	1.091	1.097	1.108	1.121	1.134	1.144	1.160	1.170	1.177
45	1.053	1.058	1.061	1.067	1.076	1.085	1.094	1.100	1.104	1.105
50	1.041	1.043	1.044	1.047	1.057	1.066	1.070	1.077	1.079	1.076
55	1.016	1.009	1.003	1.000	1.003	1.006	1.009	1.012	1.013	1.011
60	1.015	1.008	1.003	1.001	1.004	1.008	1.012	1.017	1.018	1.019
65	1.014	1.008	1.003	1.001	1.004	1.007	1.010	1.014	1.015	1.015
70	1.004	0.998	0.992	0.991	0.993	0.997	1.001	1.004	1.004	1.002
75	1.002	0.997	0.992	0.989	0.992	0.995	0.999	1.002	1.002	0.998
80	1.019	1.013	1.007	1.006	1.010	1.013	1.016	1.019	1.017	1.015
85	1.067	1.063	1.059	1.058	1.064	1.069	1.073	1.076	1.075	1.073
90	1.000	1.000	1.000	1.000	1.000	1.000	1.000	1.000	1.000	1.000

Angle (°)	Radial distance (mm)									
	5.0	5.2	5.4	5.6	5.8	6.0	6.2	6.4	6.6	6.8
0	1.314	1.349	1.385	1.422	1.484	1.523	1.587	1.657	1.698	1.793
5	1.292	1.316	1.358	1.375	1.409	1.454	1.509	1.565	1.648	1.750
10	1.309	1.330	1.359	1.388	1.419	1.460	1.507	1.567	1.642	1.718
15	1.306	1.327	1.352	1.379	1.404	1.445	1.490	1.545	1.598	1.673
20	1.291	1.308	1.328	1.350	1.379	1.410	1.454	1.502	1.556	1.622
25	1.274	1.286	1.305	1.320	1.340	1.368	1.412	1.453	1.511	1.571
30	1.245	1.256	1.268	1.282	1.301	1.324	1.362	1.404	1.446	1.498
35	1.214	1.220	1.228	1.238	1.252	1.273	1.306	1.345	1.386	1.434
40	1.184	1.188	1.192	1.195	1.203	1.262	1.280	1.290	1.315	1.365

**Table 6.** Cont.

Angle (°)	Radial distance (mm)									
	5.0	5.2	5.4	5.6	5.8	6.0	6.2	6.4	6.6	6.8
45	1.105	1.100	1.100	1.098	1.103	1.115	1.129	1.145	1.168	1.194
50	1.073	1.065	1.066	1.060	1.066	1.073	1.085	1.102	1.115	1.142
55	1.010	1.008	1.008	1.007	1.011	1.019	1.034	1.051	1.071	1.097
60	1.020	1.016	1.015	1.015	1.018	1.029	1.046	1.063	1.086	1.112
65	1.013	1.007	1.005	1.003	1.007	1.014	1.029	1.046	1.064	1.090
70	0.999	0.993	0.990	0.988	0.991	0.998	1.013	1.026	1.043	1.067
75	0.995	0.990	0.988	0.986	0.990	0.996	1.010	1.024	1.040	1.059
80	1.012	1.007	1.005	1.005	1.008	1.013	1.026	1.040	1.054	1.072
85	1.072	1.068	1.069	1.068	1.074	1.080	1.093	1.107	1.118	1.135
90	1.000	1.000	1.000	1.000	1.000	1.000	1.000	1.000	1.000	1.000

Angle (°)	Radial distance (mm)					
	7.0	7.2	7.4	7.6	7.8	8.0
0	1.928	2.086	2.210	2.389	2.640	2.913
5	1.846	1.924	2.070	2.247	2.441	2.711
10	1.810	1.920	2.050	2.177	2.358	2.582
15	1.755	1.848	1.978	2.099	2.282	2.490
20	1.700	1.806	1.898	2.015	2.173	2.365
25	1.646	1.726	1.818	1.940	2.069	2.249
30	1.552	1.638	1.711	1.818	1.927	2.098
35	1.490	1.559	1.626	1.709	1.805	1.919
40	1.410	1.464	1.522	1.597	1.663	1.781
45	1.224	1.265	1.295	1.338	1.393	1.472
50	1.155	1.182	1.216	1.252	1.293	1.357
55	1.127	1.165	1.206	1.261	1.323	1.437
60	1.144	1.179	1.220	1.275	1.336	1.458
65	1.115	1.151	1.183	1.232	1.287	1.400
70	1.087	1.118	1.145	1.190	1.237	1.347
75	1.079	1.107	1.129	1.169	1.213	1.331
80	1.090	1.114	1.134	1.171	1.214	1.328
85	1.152	1.177	1.194	1.229	1.278	1.416
90	1.000	1.000	1.000	1.000	1.000	1.000

### Anisotropy functions

In Table 6, the full data for the anisotropy functions  $F(r, \theta)$  are presented for radial distances of  $r = 1.0\text{--}8.0$  mm in 0.2-mm increments and at polar angles of  $\theta = 0^\circ\text{--}90^\circ$  in 5°-increments. The anisotropy functions for the new  $^{90}\text{Y}$  source are shown graphically for radial distances of

$r = 3.0, 4.4, 5.0, 6.0, and 7.0 mm in Figure 4. This figure shows the anisotropy function of the new  $^{90}\text{Y}$  source for most of the points,  $F(r_0, \theta_0) > 1.0$ .$

An along-away table for quality assurance (QA) purposes is presented in Table 7. For these tables, the transverse direction is equal to the  $z$  axis and the longitudinal

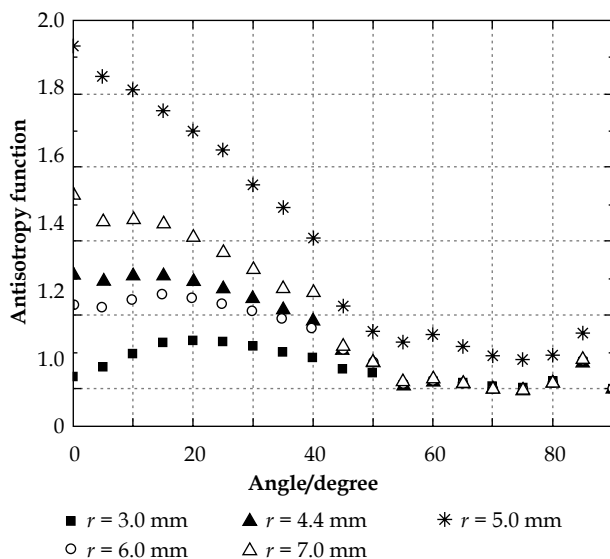


**Fig. 4.** Anisotropy function calculated for the new  $^{90}\text{Y}$  source for selected distances

direction is equal to the  $y$  axis. The new  $^{90}\text{Y}$  source is symmetric about the transverse and vertical axes. Therefore, the QA values were tabulated over the range of  $0.5 \text{ mm} \leq y \leq 8.0 \text{ mm}$  and  $0.0 \text{ mm} \leq z \leq 8.0 \text{ mm}$ .

## Conclusions

Before any of these sources can be used in clinical practice, their dosimetric parameters must be calculated by using the Monte Carlo code, which is very difficult

to perform accurately with an experimental method. Using our Monte Carlo simulation code Geant4, the dosimetric parameters for a new  $^{90}\text{Y}$  source in water have been calculated based on the dose calculation formalism recommended by the AAPM TG60 and TG149. The reference absorbed dose rate, radial dose functions, anisotropy functions, and away-along QA table were calculated for the new  $^{90}\text{Y}$  source, and the reference absorbed dose rate and radial dose functions were compared to the old  $^{90}\text{Sr}/^{90}\text{Y}$  source. Differences were observed between these two sources in terms of their energies, sizes, and materials. The new  $^{90}\text{Y}$  source had a short half-life and high energy compared with the old  $^{90}\text{Sr}/^{90}\text{Y}$  source. The parameters of this study were presented in the forms of both a graph and a table. All of the statistical uncertainties at distances for  $z \leq 8.0 \text{ mm}$  and  $y \leq 8.0 \text{ mm}$  were below 2.7%.

Our purpose in this work is to obtain the dosimetric parameters for the new  $^{90}\text{Y}$  source to be used in commercially available afterloading system in clinical practice. At present, the new  $^{90}\text{Y}$  brachytherapy source has been applied in Fonics after-loading system developed in China. According to lots of preclinical experiments for the new  $^{90}\text{Y}$  brachytherapy source by our team, this new source is well suited for radiation therapy of the liver cancer. Furthermore, these dosimetric parameters of the new  $^{90}\text{Y}$  source did not previously exist.

## Acknowledgements

This work is supported by the National Science and Technology Support Program of China (Grant Nos. 2011BAI12B05 and 2012BAI15B01).

**Table 7.** QA away-along data ( $\text{cGy min}^{-1} \text{Bq}^{-1}$ ) for the new  $^{90}\text{Y}$  source

$y/\text{mm}$	$z/\text{mm}$								
	0.0	0.5	1.0	1.5	2.0	2.5	3.0	3.5	4.0
0.5	36.8321	36.5824	35.5580	33.0367	26.1714	13.5173	6.1762	3.3402	1.9918
1.0	14.9909	14.7572	13.9972	12.5610	10.0844	6.9074	4.2817	2.6675	1.7099
1.5	8.1914	8.0193	7.5110	6.6695	5.5092	4.2342	2.9353	2.0079	1.4106
2.0	4.9825	4.8483	4.5334	4.0338	3.4125	2.7925	2.0564	1.4964	1.1129
2.5	3.1924	3.0949	2.8955	2.5930	2.2365	1.9024	1.4499	1.0993	0.8513
3.0	2.0988	2.0393	1.9032	1.7172	1.5041	1.3117	1.0228	0.7979	0.6358
3.5	1.3942	1.3710	1.2691	1.1522	1.0217	0.9071	0.7187	0.5712	0.4624
4.0	0.9591	0.9186	0.8484	0.7751	0.6953	0.6205	0.4989	0.4028	0.3279
4.5	0.6210	0.6145	0.5648	0.5185	0.4698	0.4184	0.3406	0.2784	0.2279
5.0	0.4309	0.4101	0.3731	0.3431	0.3135	0.2778	0.2277	0.1876	0.1538
5.5	0.2702	0.2711	0.2428	0.2232	0.2054	0.1800	0.1482	0.1230	0.1006
6.0	0.1849	0.1746	0.1534	0.1417	0.1311	0.1126	0.0932	0.0777	0.0623
6.5	0.1042	0.1075	0.0932	0.0870	0.0806	0.0669	0.0561	0.0469	0.0366
7.0	0.0677	0.0631	0.0541	0.0509	0.0474	0.0376	0.0320	0.0268	0.0202
7.5	0.0326	0.0348	0.0298	0.0282	0.0264	0.0199	0.0171	0.0144	0.0104
8.0	0.0195	0.0178	0.0151	0.0146	0.0136	0.0097	0.0084	0.0071	0.0048

**Table 7.** Cont.

y/mm	z/mm							
	4.5	5.0	5.5	6.0	6.5	7.0	7.5	8.0
0.5	1.2519	0.8145	0.5393	0.3541	0.2313	0.1482	0.0936	0.0574
1.0	1.0843	0.7146	0.4754	0.2992	0.1938	0.1234	0.0722	0.0437
1.5	0.9175	0.6137	0.4238	0.2648	0.1711	0.1119	0.0643	0.0385
2.0	0.7482	0.5134	0.3589	0.2271	0.1478	0.0969	0.0558	0.0333
2.5	0.5871	0.4131	0.2915	0.1861	0.1225	0.0805	0.0465	0.0277
3.0	0.4475	0.3205	0.2275	0.1469	0.0976	0.0641	0.0371	0.0221
3.5	0.3311	0.2412	0.1726	0.1114	0.0743	0.0491	0.0283	0.0167
4.0	0.2380	0.1758	0.1262	0.0818	0.0547	0.0357	0.0205	0.0122
4.5	0.1662	0.1238	0.0888	0.0576	0.0385	0.0249	0.0144	0.0084
5.0	0.1127	0.0841	0.0597	0.0390	0.0260	0.0165	0.0094	0.0054
5.5	0.0739	0.0552	0.0384	0.0252	0.0167	0.0103	0.0059	0.0033
6.0	0.0462	0.0345	0.0233	0.0154	0.0102	0.0061	0.0034	0.0019
6.5	0.0275	0.0203	0.0134	0.0088	0.0058	0.0033	0.0018	0.0010
7.0	0.0152	0.0113	0.0072	0.0047	0.0030	0.0017	0.0009	0.0005
7.5	0.0078	0.0058	0.0036	0.0023	0.0015	0.0008	0.0004	0.0002
8.0	0.0037	0.0027	0.0016	0.0010	0.0006	0.0003	0.0002	0.0001

## Disclosure

Authors report no conflict of interest.

## References

- Soares CG, Halpern DG, Wang CK et al. Calibration and characterization of beta-particle sources for intravascular brachytherapy. *Med Phys* 1998; 25: 339-346.
- Holmes SM, DeWerd LA, Micka JA. Experimental determination of the radial dose function of  $^{90}\text{Sr}/^{90}\text{Y}$  IVBT sources. *Med Phys* 2006; 34: 3225-3233.
- Nelson K, Vause PE Jr, Koropova P. Post-mortem considerations of Yttrium-90 ( $^{90}\text{Y}$ ) microsphere therapy procedures. *Health Phys* 2008; 95 (5 Suppl): S156-161.
- Cohen G, Munro JJ 3rd, Kirov A et al.  $^{32}\text{P}$  brachytherapy conformal source model RIC-100 for high-dose-rate treatment of superficial disease: Monte Carlo calculations, diode measurements, and clinical implementation. *Int J Radiat Oncol Biol Phys* 2014; 88: 746-752.
- Nath R, Amols H, Coffey C et al. Intravascular brachytherapy physics: Report of the AAPM Radiation Therapy Committee Task Group no. 60. American Association of Physicists in Medicine. *Phys Med* 1999; 26: 119-152.
- Chiu-Tsao S, Schaart DR, Soares CG et al. Dose calculation formalisms and consensus parameters for intravascular brachytherapy: Recommendations of the AAPM Radiation Therapy Committee Task Group No. 149. *Med Phys* 2007; 34: 4126-4158.
- Asenjo J, Fernández-Varea JM, Sánchez-Reyes A. Characterization of a high-dose-rate  $^{90}\text{Sr}-^{90}\text{Y}$  source for intravascular brachytherapy by using the Monte Carlo code PENELOPE. *Phys Med Biol* 2002; 47: 697-711.
- Wang R, Li XA. A Monte Carlo calculation of dosimetric parameters of  $^{90}\text{Sr}/^{90}\text{Y}$  and  $^{192}\text{Ir}$  SS sources for intravascular brachytherapy. *Med Phys* 2000; 27: 2528-2535.
- Andreo P. Monte Carlo techniques in medical radiation physics. *Phys Med Biol* 1991; 36: 861-920.
- Karimian A, Saghamanesh S. A dosimetry evaluation of  $^{90}\text{Y}$ -stent implantation in intracoronary radiation treatment. *Nucl Techn Radiat Protect* 2013; 28: 278-283.
- Cross W, Ing H, Freedman N et al. A short atlas of beta-ray spectra. *Phys Med Biol* 1983; 28: 1251-1260.
- Walichiewicz P, Petelenz B, Wilczek K et al.  $^{32}\text{P}$  liquid sources - comparison of the effectiveness of postangioplasty versus poststenting intravascular brachytherapy in hypercholesterolemic rabbits. Adjunctly implanted titanium stent does not attenuate the effect of endovascular irradiation. *Cardiovasc Radiat Med* 2003; 4: 64-68.
- Agostinelli S, Allison J, Amako K et al. GEANT4 Collaboration. Geant4 - a simulation toolkit. *Nucl Instrum Meth A* 2003; 506: 250-303.
- Ballarini F, Battistoni G, Campanella M et al. The FLUKA code: an overview. *J Phys Confer Series* 2006; 41: 151-160.
- Wang R, Sloboda RS. EGS4 dosimetry calculation for cylindrically symmetric brachytherapy sources. *Med Phys* 1996; 23: 1459-1465.
- Chiu-Tsao S, Fang FX, Ahumbay E et al. Dosimetric parameters for  $^{192}\text{I}$  and  $^{125}\text{I}$  seeds for intravascular brachytherapy. *Med Phys* 1997; 24: 1994.
- Asenjo J, Fernández-Varea JM, Sánchez-Reyes A. Characterization of a high-dose-rate  $^{90}\text{Sr}-^{90}\text{Y}$  source for intravascular brachytherapy by using the Monte Carlo code PENELOPE. *Phys Med Biol* 2002; 47: 697-711.
- Torres J, Buades MJ, Almansa JF et al. Dosimetry characterization of  $^{32}\text{P}$  intravascular brachytherapy source wires us-

- ing Monte Carlo codes PENELOPE and GEANT4. *Med Phys* 2004; 31: 296-304.
- 19. Cullen DE, Hubbell JH, Kissel L et al. EPDL97: the Evaluated Photon Data Library, '97 Version. University of California, Lawrence Livermore National Laboratory, Livermore, 1997.
  - 20. Cullen DE, Perkins ST, Seltzer SM et al. Tables and graphs of electron-interaction cross-sections from 10 eV to 100 GeV derived from the LLNL Evaluated Electron Data Library (EEDL), Z = 1 - 100. Livermore National Laboratory, Lawrence 2001.
  - 21. Mardirossian G, Hall M, Montebello J et al. Dose distribution to spinal structures from intrathecally administered yttrium-90. *Phys Med Biol* 2006; 51: 185-196.
  - 22. Rivard M, Coursey B, DeWerd L et al. Update of AAPM Task Group No. 43 Report: A revised AAPM protocol for brachytherapy dose calculations. *Med Phys* 2004; 31: 633-674.